

Pamiparib is a potent and selective PARP inhibitor with unique potential for the treatment of brain tumor



Yao Xiong^a; Yin Guo^b; Ye Liu^c; Hexiang Wang^d; Wenfeng Gong^a; Yong Liu^a; Xing Wang^a; Yajuan Gao^a; Fenglong Yu^a; Dan Su^e; Fan Wang^a; Yutong Zhu^b; Yuan Zhao^b; Yiyuan Wu^b; Zhen Qin^b; Xuebing Sun^c; Bo Ren^d; Bin Jiang^f; Wei Jin^f; Zhirong Shen^f; Zhiyu Tang^g; Xiaomin Song^a; Lai Wang^a; Xuesong Liu^b; Changyou Zhou^d; Beibei Jiang^{a,*}

^aDepartment of In Vivo Pharmacology, BeiGene (Beijing) Co., Ltd., Beijing, PR China; ^bDepartment of Discovery Biology, BeiGene (Beijing) Co., Ltd., Beijing, PR China; ^cDepartment of Biochemistry, BeiGene (Beijing) Co., Ltd., Beijing, PR China; ^dDepartment of Chemistry, BeiGene (Beijing) Co., Ltd., Beijing, PR China; ^eDepartment of DMPK, BeiGene (Beijing) Co., Ltd., Beijing, PR China; ^fDepartment of Discovery Biomarkers, BeiGene (Beijing) Co., Ltd., Beijing, PR China; ^gDepartment of Clinic Pharmacology, BeiGene (Beijing) Co., Ltd., Beijing, PR China

Abstract

Pamiparib, an investigational Poly (ADP-ribose) polymerase (PARP) inhibitor in clinical development, demonstrates excellent selectivity for both PARP1 and PARP2, and superb anti-proliferation activities in tumor cell lines with BRCA1/2 mutations or HR pathway deficiency (HRD). Pamiparib has good bioavailability and is 16-fold more potent than olaparib in an efficacy study using BRCA1 mutated MDA-MB-436 breast cancer xenograft model. Pamiparib also shows strong anti-tumor synergy with temozolomide (TMZ), a DNA alkylating agent used to treat brain tumors. Compared to other PARP inhibitors, pamiparib demonstrated improved penetration across the blood brain barrier (BBB) in mice. Oral administration of pamiparib at a dose as low as 3 mg/kg is sufficient to abrogate PARylation in brain tumor tissues. In SCLC-derived, TMZ-resistant H209 intracranial xenograft model, combination of pamiparib with TMZ overcomes its resistance and shows significant tumor inhibitory effects and prolonged life span. Our data suggests that combination of pamiparib with TMZ has unique potential for treatment of brain tumors. Currently, the combination therapy of pamiparib with TMZ is evaluated in clinical trial [NCT03150862].

Neoplasia (2020) 22 431–440

Keywords: Pamiparib, PARP, TMZ, Brain penetration

Introduction

Genomic instability is a hallmark of cancer that drives tumorigenesis and progression [1]. Specifically, in familial cancers, mutations in the BRCA1 and BRCA2 tumor suppressor genes, or in genes essential for homologous recombination (HR), have been associated with an increased risk of breast or ovarian cancer development [2]. Mutations in BRCA1 or BRCA2 predispose women to hereditary breast and ovarian cancers, which account for 3–5% of all breast cancers, and a greater proportion of ovarian cancers [3]. Poly (ADP-ribose) polymerase (PARP) is an enzyme involved in the base excision repair (BER) pathway that regulates DNA single-strand breaks (SSB) repairment [4,5]. Several studies have shown that BRCA-deficient cells, and more broadly, cells with HR deficiency

(HRD), appear to be highly sensitive to PARP inhibition [6–9]. Two studies [10,11] have reported that treatment with PARP inhibitor alone could kill tumor cells—and especially cells with BRCA1/2 mutations—in the absence of exogenous DNA-damaging agents. Preclinical studies further confirmed that PARP inhibition can induce the accumulation of unrepaired DNA SSB, resulting in synthetic lethality in cancer cells with BRCA1 and BRCA2 mutations, supporting that PARP inhibitors are promising agents for treatment of tumors harboring BRCA1/2 mutations [12].

In clinical applications, PARP inhibitors, including olaparib, rucaparib, niraparib, and talazoparib, have demonstrated sustained anti-tumor responses as single agents in patients with BRCA1- or BRCA2-

* Corresponding author at: BeiGene (Beijing) Co., Ltd., No. 30 Science Park Road, Zhong-Guan-Cun Life Science Park, Changping District, Beijing 102206, PR China. e-mail address: beibei.jiang@beigene.com (B. Jiang).

mutations [13–17]. PARP inhibitors can potentiate efficacy of genotoxic agents such as DNA alkylating agents, by disruption of BER in the DNA repair pathway [18]. Thus, another direction for PARP inhibitors in clinical development is their combination with chemotherapies [15]. Temozolomide (TMZ) is an oral alkylating agent that activates DNA repair. At physiological pH, TMZ is chemically converted to MTIC (5–3-(methyltriazen-1-yl)imidazole-4-carboximide) and degrades to a methyl diazonium cation that can transfer a methyl group to DNA. Methylation on O6-MeG can be repaired by DNA-repair protein O6 methylguanine-DNA methyltransferase (MGMT) without cytotoxicity. However, when MGMT is inactivated or cannot completely repair O6-MeG, cytotoxicity is induced: TMZ triggers apoptosis [19–21]. One well-defined mechanism of TMZ resistance is through the PARP-dependent BER pathway [22,23]. It is therefore conceivable that PARP inhibitors may potentiate the efficacy of TMZ, especially in a TMZ-resistant background. Previous studies have demonstrated sufficient brain penetration as a prerequisite for the efficacy of PARP inhibitors in glioma tumors or other tumors with brain metastasis [24]. Unfortunately, P-glycoprotein (P-gp) and breast cancer resistance protein (BCRP), which function as efflux pumps at the blood brain barrier (BBB), are known to limit brain penetration of multiple PARP inhibitors, thereby hindering the anti-tumor efficacy of earlier generations of PARP inhibitors like olaparib, rucaparib, talazoparib, and veliparib [25,26].

In this study, we report the discovery of a novel PARP1/2 inhibitor pamiparib with good selectivity and PK profile. The anti-tumor efficacy of pamiparib alone or combined with TMZ in several primary or resistant tumor models were evaluated. Pamiparib is a not a substrate of P-gp or BCRP. With its high penetration across the BBB, pamiparib exerted strong synergy with TMZ in intracranial tumor models, including a TMZ-resistant model. Collectively, our results strongly support the clinical development of pamiparib as a combination regimen with TMZ to treat patients with brain tumors, especially those that are resistant to TMZ alone.

Materials and methods

Enzyme inhibitory assay

Pamiparib was tested for PARP1, PARP2, PARP3, TNKS1 and TNKS2 inhibition using commercial PARP or TNKS Chemiluminescent Assay Kits (BPS Bioscience Inc.), and following the manufacturer's instructions. Briefly, histones were immobilized on the surface of high binding plates and then incubated with serial dilutions of compounds and the targeted PARP enzyme for 0.5 hr. Biotinylated NAD and activating DNA were added to initiate the reactions. After 1 h at room temperature, the reactions were terminated by removing reaction mixtures from the wells. The biotinylated PARylation products on immobilized histones were quantified by linking to streptavidin-HRP and measured using a chemiluminescent HRP reaction. Chemiluminescence was measured on a PHERAstar FS plate reader or a FLUOstar OMEGA (BMG LAB-TECH). The IC₅₀ values were calculated based on inhibition of enzyme activity in the presence of increasing concentrations of compounds. IC₅₀s of pamiparib for PARP6, PARP7, PARP8, PARP10, PARP11 and PARP12 were tested by BPS Bioscience Inc.

DNA trapping activity

Pamiparib was tested for DNA trapping activity using a fluorescence polarization (FP) method [8]. PARP1 enzyme and serial dilutions of compounds were added to the 384 well plate. DNA labeled with 5'-Alexa Fluor 488 containing a nick and a 5'-dRP at the nicked site was added and incubated for 0.5 h at room temperature. NAD was added to the wells to initiate the PARylation reactions. PARylation reduced the FP signal by

freeing the DNA from PARP1. After a 1 h reaction at room temperature, FP values were measured on a PHERAstar FS plate reader (BMG LAB-TECH). The EC₅₀ values were calculated based on inhibition of FP signal changes as a function of increasing concentrations of compounds.

Cell lines and cell culture

A panel of breast, ovarian, colon, lung, and pancreatic cancers and medulloblastoma cell lines were used in this study. All cancer cell lines were maintained in Dulbecco's modified Eagle medium (DMEM, Gibco); Iscove's modified Dulbecco's medium (IMDM); McCoy's 5A; or RPMI-1640 supplemented with 10% FBS (Thermo Scientific), 100 units/ml penicillin, and 0.1 mg/ml streptomycin; the unspecified cell culture reagents were obtained from Life Technologies. Cell lines were kept at 37 °C in a humidified atmosphere of 5% CO₂ in air. Cell lines were revived from frozen stocks that were laid down within three passages from the original cells purchased.

Inhibition of H₂O₂-induced PAR synthesis in HeLa and glioma cells

Tumor cells were seeded into a 96-well plate with a clear bottom and black wall at an initial concentration of 5000 cells/well in culture medium (100 µL DMEM containing 10% FBS, 0.1 mg/mL penicillin–streptomycin). After 4 h compounds were added into the cell culture with eight serial dilutions over a 0.02–200 nM final concentration range in 0.1% DMSO/culture medium. Eighteen hours of compound treatment was followed by induction of DNA damage with 200 µM of H₂O₂ solution at 37 °C for 5 min. The cells were further fixed with 100 µL/well of ice-cold methanol at –20 °C for 20 min. After fixation and a brief wash, the cells were stained in detection buffer (50 µL/well, containing PBS, Tween (0.1%), and BSA (1 mg/mL)) containing the primary PAR mAb (Alexis ALX-804-220, 1:2000), the secondary anti-mouse Alexa Fluor 488 antibody (Molecular Probes A11029, 1:2000), and nuclear dye DAPI (Molecular Probes D3571, 150 nM) at 4 °C overnight in the dark. The signals of Alexa 488-stained PAR polymer and the signals of DAPI-stained nuclei were captured on an ArrayScan VTI (ThermoFisher). The mean of total intensity of cells was calculated by measuring the average of total intensity of nuclei over the total number of DAPI-labeled nuclei. The IC₅₀ was determined based on the residual enzyme activity in the presence of increasing amounts of PARP inhibitors.

Cell proliferation inhibitory test

The growth-inhibitory activity of compounds in a panel of breast, ovarian, colon, and lung cancer cell lines were determined using a CellTiter-Glo luminescent cell viability assay (Promega). The number of cells seeded per well of a 96-well plate was optimized for each cell line to ensure logarithmic growth over the 7-day treatment period. Cells were left to attach for 16 h; cells were treated in duplicate with a 10-point dilution series. Following 7 days of exposure to the compound, a volume of CellTiter-Glo reagent equal to the volume of cell culture medium present in each well was added. The plate was then mixed on an orbital shaker for 2 min to allow cell lysis, followed by a 10-min incubation at room temperature to allow development and stabilization of luminescent signal, which corresponded to quantity of ATP and thus the quantity of metabolically active cells. Luminescent signal was measured using PHERAstar FS reader (BMG Labtech). Cell viability was expressed relative to mock treatment control.

Xenograft models

All animal studies were carried out in accordance with the Institutional Animal Care and Use Committee (IACUC) of BeiGene. MDA-MB-436 cells were prepared at the concentration of 2.5×10^7 cells/mL in 1:1 PBS and Matrigel (BD). Cell suspension (0.2 ml) was implanted subcutaneously on the right front flank of 6–8 weeks old female BALB/c nude mice (Beijing HFK Bioscience Co., Ltd). When average tumor size reached $\sim 130 \text{ mm}^3$, mice were assigned to six groups with nine mice per group using a stratified randomization procedure. Mice were orally administrated twice daily (BID) with vehicle (0.5% methylcellulose (MC)), 1.6, 3.1, 6.3 mg/kg pamiparib, or 25, 50 mg/kg olaparib for 28 days, respectively.

Small cell lung cancer cell line H209 and its TMZ resistant cell line H209-TR were used to evaluate combined TMZ and pamiparib efficacy. H209-TR (TMZ-resistant) cells were generated from H209 tumors by treating with multiple cycles of TMZ *in vivo*. For H209 and H209TR xenograft establishment, cells were prepared at the concentration of 2×10^5 cells/mL in PBS and 0.2 ml of cell suspension was implanted subcutaneously in the right flank of 6–8 weeks old female BALB/c nude mice. When average tumor size reached $\sim 200 \text{ mm}^3$, mice were assigned to four groups with seven mice per group using a stratified randomization procedure. Mice were treated twice daily (BID) with vehicle (0.5% methylcellulose (MC)), 3 mg/kg pamiparib for 28 days, or 50 mg/kg TMZ once per day and combination of these two agents for the first 5 days in a three-week cycle; a total of three cycles of TMZ were given during the whole treatment schedule, or in combination with pamiparib.

Mice with established intracranial H209 xenografts were used to investigate the combined activity of pamiparib and TMZ on tumors grown in the brain. BALB/c nude mice were anesthetized with an intraperitoneal injection of Avertin (300 mg/kg, working concentration 2.5%). The surgical site was shaved and prepared with iodine and 70% ethyl alcohol. A midline incision was made, followed by injection of 3×10^5 H209 or H209TR cells in 2 μL PBS into the right brain. Three days after inoculation, animals were randomized into four groups with 16 animals in each group. Mice were treated twice daily (BID) with vehicle (0.5% methylcellulose (MC)), 3 mg/kg pamiparib for 28 days, 50 mg/kg TMZ once per day for 5 days, or a combination of pamiparib and TMZ. Mice body weights were measured twice a week, and mice were sacrificed once they lost over 20% of their body weight.

Pharmacokinetics (PK) and pharmacodynamics (PD) study

MDA-MB-436 xenograft was used for mice PK and PD study. When the average tumor size reached 200–600 mm^3 , animals were assigned to 14 groups with four mice per group using a stratified randomization procedure. Seven groups of mice were treated with 5.45 mg/kg of pamiparib and animals were euthanized at 0.5, 1, 2, 4, 8, 12 and 24 h after dosing. The other seven groups of mice were treated with vehicle (0.5% methylcellulose (MC)) alone, 0.17, 0.34, 0.68, 1.36, 2.73, 5.45 or 10.90 mg/kg of pamiparib. Animals were euthanized 4 h after dosing. All doses were based on free base weight. At the indicated time points, mice were euthanized using carbon dioxide; plasma and tumor samples were collected and stored at -80°C freezer for further PK/PD analysis. A similar PD study was also conducted in MDA-MB-436 xenografts, for pamiparib PD effect compared with olaparib. Briefly, six groups with eight mice per group were included. Each group of mice was treated with 0.15, 0.5 and 1.5 mg/kg pamiparib or 2.5, 7.5 and 25 mg/kg olaparib, and the mice were euthanized at 0.5 and 12 h after dosing.

The bioanalysis of pamiparib in mouse plasma and tumor samples was analyzed at 3D BioOptima Co., Ltd. (Suzhou, China). After protein precipitation with acetonitrile containing an internal standard and centrifuga-

tion at 14,000 rpm for 8 min, pamiparib levels in plasma and tumor tissues were determined by LC-MS/MS (Applied Biosystems, API 4000-Qtrap). The dosing solutions used for the last dose were analyzed to determine the actual dose administered.

The PD activity of pamiparib was examined by determining PAR concentrations in tumor homogenates with an HT PARP *in vivo* pharmacodynamic assay II (Trevigen, Cat# 4520-096-K). Two μg of protein lysates were added to measure PAR level following the kit's instructions. PAR levels are expressed in terms of pg/ml per 100 μg /ml xenograft extract.

The rat and dog PK studies were analyzed at 3D BioOptima Co., Ltd. (Suzhou, China). After protein precipitation with acetonitrile containing an internal standard and centrifugation at 14,000 rpm for 8 min, pamiparib levels in plasma and tumor tissues were determined by LC-MS/MS (Applied Biosystems, API 4000-Qtrap). The dosing solutions used were analyzed to determine the actual dose administered.

Brain penetration study

Central nervous system tissue distribution of pamiparib was determined by WuXi AppTec (Cranbury, NJ, USA). Quantitative whole-body autoradiography (QWBA) was used to determine the tissue distribution following a single oral gavage (PO) administration of 5 mg/kg (100 $\mu\text{Ci}/\text{kg}$) of [^{14}C] pamiparib to male Long-Evans or Sprague-Dawley rats. The brain penetration of pamiparib in male C57 mice and rats were evaluated after a single administration of pamiparib (PO 10 mg/kg in mice or IV 1 mg/kg in rat). Three groups of animals were euthanized at indicated time points (1 h, 2 h, and 4 h for mice or 0.083 h, 1 h and 2 h for rats) after dosing. Blood was collected via cardiac puncture, brain was collected, washed with ice-cold saline and homogenized in ice cold PBS or 20% methanol in water. The concentrations of pamiparib in plasma and brain were determined by LC-MS/MS. Based on brain protein binding and plasma protein binding data (data not shown), the brain to plasma unbound partition coefficient (K_{puu}) was determined to measure the potency of a compound penetration in brain as follows:

$K_{\text{puu}} = \text{free drug concentration in brain} / \text{free drug concentration in plasma}$

Statistical analysis

All data are presented as mean \pm standard error of the mean (SEM) from three independent repeated experiments. The differences between the mean values of data for comparing groups were analyzed for significance using the one-way ANOVA by GraphPad Prism; $P \leq 0.05$ was considered statistically significant.

Results

Pamiparib inhibits PARP enzyme activity and cellular PARylation

The chemical structure of pamiparib is shown in Fig. 1A. Pamiparib is a potent PARP1/2 inhibitor, for which it has respective IC_{50} values of 1.3 or 0.92 nM. Pamiparib was also tested against PARP3, tankyrase1/2, and other PARP isoforms (Fig. 1B), and found to be less active or inactive, with IC_{50} values more than 50–100-fold higher. These data indicate that pamiparib is a potent and selective PARP1/2 inhibitor. In light of the hypothesis that trapping PARP1/2 on damaged DNA mechanistically contributes to the cytotoxicity of PARP inhibitors, we measured the capacity for pamiparib to trap PARP1–DNA complexes. We found that pamiparib showed strong DNA-trapping activity, with an EC_{50} of 13 nM. Cellular assays confirmed that pamiparib can inhibit intracellular PARP activity in H_2O_2 -treated HeLa cells in a dose-dependent manner, with an IC_{50} of 0.24 nM (Fig. 1C).

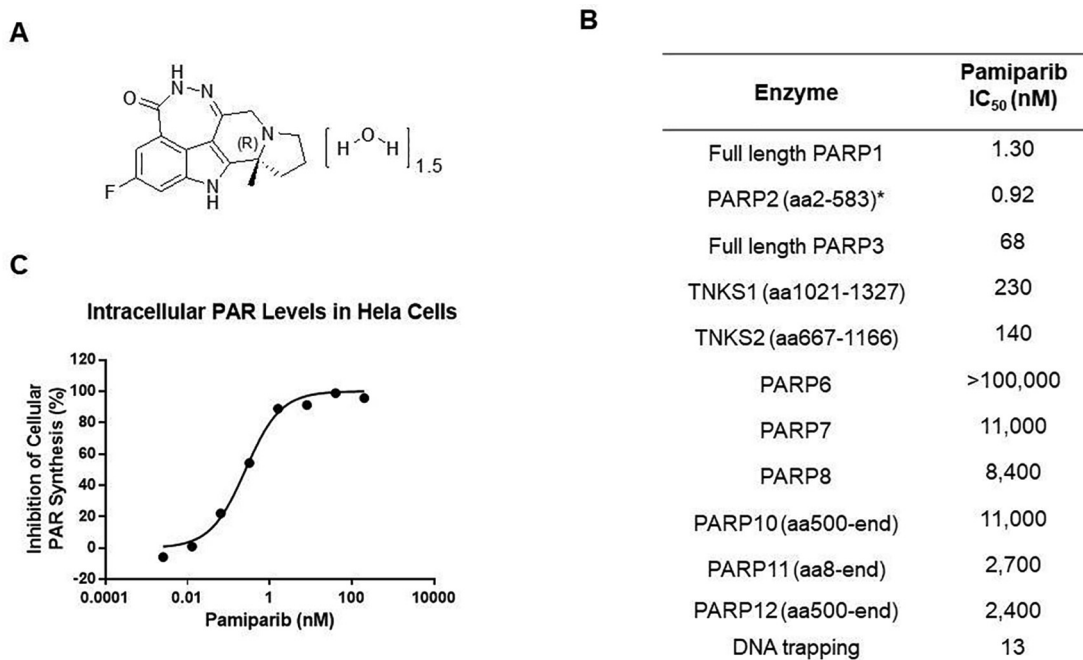


Fig. 1. The structural of Pamiparib and its activity. (A) The chemical structure of pamiparib. (B) The inhibitory effect of pamiparib on PARP enzymes. (C) The efficacy of pamiparib against intracellular PAR levels in HeLa cells. HeLa cells were incubated with the indicated concentrations of pamiparib for 18 hrs, and then cells were exposed to hydrogen peroxide (H_2O_2) to induce PAR synthesis. PAR levels without H_2O_2 induction were set as 100%.

Pamiparib specifically inhibits the proliferation of cancer cells with HR-deficiency or BRCA mutations

To investigate the activity and selectivity of pamiparib, we next evaluated the anti-proliferation activity of pamiparib in different cancer cell lines. Tumor cell lines that were either BRCA1-deficient (MDA-MB-436 and UWB1.289) or BRCA2-deficient (Capan-1) were highly sensitive to pamiparib, while BRCA wild-type cell line (MDA-MB-231) was resistant to pamiparib (Fig. 2A). PTEN mutation/loss has been shown previously to cause a deficiency in HR pathways and induce sensitivity to PARP1/2 inhibitors [27], and we found that pamiparib was approximately 13-fold more potent in inhibiting PTEN deficient (MEF/PTEN $-/-$) cells than sufficient (MEF/PTEN $+/-$) ones. The antiproliferation activities of pamiparib and olaparib were then evaluated head-to-head using several tumor cell lines (Supplementary Table 1). Similar to olaparib, pamiparib potently and selectively inhibited cell lines with known HRD such as MDA-MB-436, HCC1395, UWB1.289, and HCT116/ATR(-/ flox); in contrast, pamiparib did not effectively inhibit other cancer cells that demonstrated HRD (Fig. 2A and Supplementary Table 1). These observations were consistent with the mechanism of action reported for other known PARP inhibitors [10,11]. Taken together, these results indicate that pamiparib functions as a potent anti-tumor agent with strong selectivity for tumors that harbor HRD and BRCA mutations.

PK and PD studies reveal high bioavailability and sustained activity of pamiparib in animal models

To further characterize the pharmacokinetic (PK) properties of pamiparib, its exposure was evaluated in healthy mice, rat, and dog at 10, 5, 2 mg/kg p.o. or 1, 2, 1 mg/kg *i.v.* doses, respectively (Table 1). Based on dose titration or time-dependent pharmacodynamic (PD) studies, as well as efficacy studies (Fig. 3), a simple PK/PD model was established to help understand the relationship between pamiparib dose and efficacy.

The model indicated that only doses higher than 5.45 mg/mL can induce $\geq 80\%$ PAR inhibition (Fig. 3C); at this dosage, the intra-tumor concentration is around 0.8 $\mu\text{mol/kg}$. Based on this finding, we conducted a time-dependent PD assessment after a single dose of 5.45 mg/mL (Fig. 3D). At 5.45 mg/mL, pamiparib induced rapid and potent inhibition of PARylation. This inhibition was 98% at 0.5 h post treatment and remained high ($\geq 80\%$) through the first 12 h; however, the PARylation inhibition dropped to 53% at 24 h after treatment. These data were well-correlated with the changes in pamiparib concentrations that are detected in tumor sites and in plasma (Fig. 3D). The intra-tumor concentration of pamiparib remained at high level ($>0.5 \mu\text{mol/kg}$) in the first 12 h, and dropped gradually afterwards to its minimum at 24 h. Together, these results suggest that an intra-tumor concentration of $>0.5 \mu\text{mol/kg}$ is needed to achieve at least 80% PARylation inhibition by pamiparib, and a two-dose-a-day regimen (BID dosing) will be suitable for efficacy studies to maintain sufficient PD effects in mice.

Pamiparib is more potent than olaparib in the HR-deficiency xenograft model in vivo

To further evaluate the *in vivo* efficacy, a BRCA1 mutant MDA-MB-436 xenograft breast cancer model was established and tested with pamiparib, doses ranging from 1.6 mg/kg to 6.3 mg/kg (oral, BID for 28 days). Pamiparib induced tumor regression on day 29 and resulted in 100% objective responses (Fig. 3A). At day 89, two months after the treatment was terminated, tumor relapse was observed in the mice treated with olaparib 25 mg/kg BID and pamiparib at the lowest dose (1.6 mg/kg). No body weight loss was observed during the treatment (Fig. 3B).

Then, the PD effect of pamiparib was evaluated *in vivo* by directly measurement of PAR level in tumor site. MDA-MB-436 xenograft mice were treated once orally with the vehicle or pamiparib, at a dose ranging from 0.17 to 10.9 mg/kg. The concentration of pamiparib in serum or at the tumor site increased proportionally with dose and positively

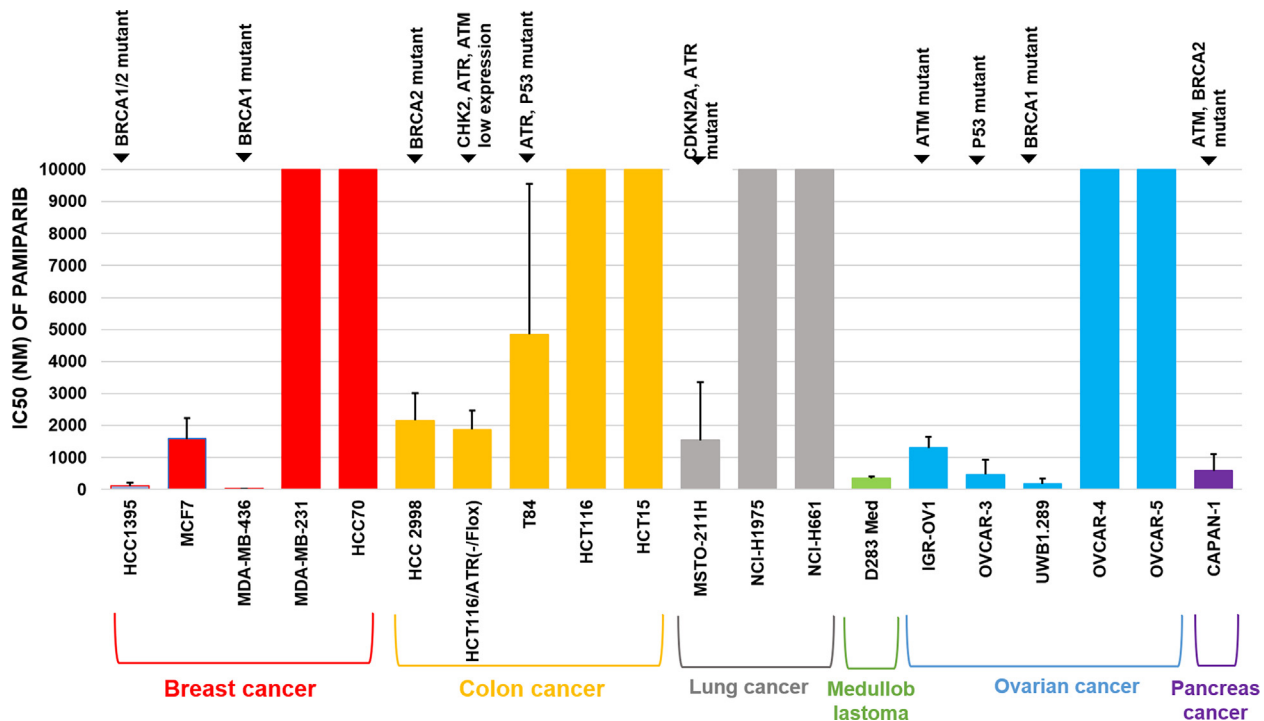


Fig. 2. Pamiparib shows specific growth inhibitory effects in HR deficient and BRAC mutant cell lines. (A) The anti-proliferative activity of pamiparib in several tumor cell lines. IC₅₀ values indicate that pamiparib potently inhibited the tumor cells with HR-deficiency or BRAC mutants. For all experiments, viability was derived after 7 days of continuous treatment with pamiparib.

Table 1. PK parameters of Pamiparib.

Species	$T_{1/2}$ (h)	AUC _{0-inf} /Dose (ng·h/mL per mg/kg)	Clearance (mL/kg/min)	Vdss (L/kg)	F (%)
Mouse	3.2 ± 0.5	552 ± 194	29.9 ± 2.4	5.7 ± 0.5	99 ± 35
Rat	5.5 ± 0.8	694 ± 124	22.7 ± 2.8	6.9 ± 0.7	94 ± 17
Dog	3.6 ± 1.9	800 ± 95	15.2 ± 1.0	2.1 ± 0.2	73 ± 4.0

correlated with the extent of PAR inhibition in tumors (Fig. 3C). Moreover, a single dose of 5.45 mg/kg led to rapid and pronounced decrease in PAR levels in a time-dependent manner (Fig. 3D): the PARylation inhibition was 98% at 0.5 h after treatment, remained high (>80%) throughout the first 12 h, and then dropped to 53% at 24 h post treatment.

Next the PD and efficacies of pamiparib and olaparib was compared head-to-head in the same model. A single dose of pamiparib at 1.5 mg/kg induced 89% PARylation inhibition at 0.5 h post treatment which remained at ~81% throughout the first 12 h. Meanwhile a single dose of olaparib at 25 mg/kg induced ~100% PARylation inhibition but dropped to 72% by 12 h post treatment. These data suggest that compared to olaparib, the induction of PAR inhibition by pamiparib lasts longer at tumor sites (Fig. 3E). In comparisons of efficacy, pamiparib induced tumor regression on day 29, resulting in 100% objective responses at the lowest dose (1.6 mg/kg). In contrast, olaparib induced tumor regression at both doses tested (25 and 50 mg/kg, BID), but only achieved 100% objective responses in the high-dose group. Tumor progression was monitored for two additional months after cessation of dosing. On Day 89, tumor relapse of the tumor was apparent in the low-dose groups, with olaparib at 25 mg/kg BID being the least effective, followed by pamiparib at 1.6 mg/kg BID (Fig. 3A). These results suggest that pamiparib exhibits approximately 16-fold higher efficacy than olaparib in this model, likely due to higher drug exposure in body.

Pamiparib potentiates the anti-proliferation effects of TMZ in glioblastoma multiforme (GBM) and small cell lung cancer (SCLC) cells.

TMZ, a DNA alkylating agent, is currently used for treating several malignancies, including GBM and SCLC with brain metastasis [28,29]. PARP inhibitors have been reported to potentiate TMZ by disrupting BER in the DNA repair pathway. To determine if pamiparib also potentiates the effect of TMZ, we explored the combined effects of pamiparib and TMZ in 8 GBM and 7 SCLC cell lines. The anti-proliferative synergy was assessed by the Excess over Bliss (EOB), which determines whether the combined effect of the two compounds is significantly greater or smaller than the naïve (independent) combination of their individual effects; an EOB ≥ 10 typically indicates synergy [30]. Pamiparib demonstrated synergism with TMZ in 7 GBM and 4 SCLC cell lines, with an average EOB value of 24.8 and 17.9, respectively (Table 2). The maximum EC₅₀ of TMZ when combined with pamiparib was more than 5-fold higher than that of TMZ alone in all cell lines, with a >33-fold shift in the most strongly affected cell line. Cellular assays further confirmed that pamiparib can inhibit intracellular PARP activity in H₂O₂-treated glioma cells SF-295 and GL261 in a dose-dependent manner, with IC₅₀s of 0.17 and 0.25 nM (Supplementary Fig. 3), respectively. The combination effect of pamiparib with TMZ has also been tested in additional 11 gastric

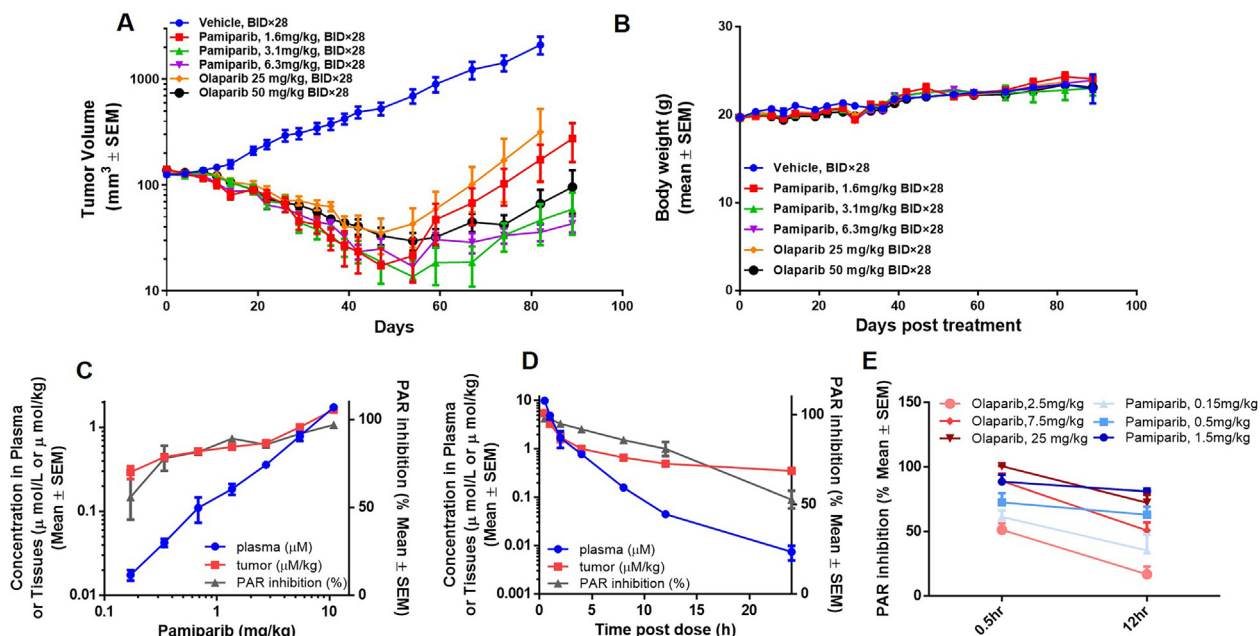


Fig. 3. *In vivo* efficacy, PK and PD of pamiparib in a human MDA-MB-436 breast cancer xenograft model. (A) *In vivo* efficacy of pamiparib and olaparib was head-to-head compared in a human MDA-MB-436 breast cancer xenograft model. Doses ranging from 1.6 mg/kg to 12.5 mg/kg of pamiparib and 25 mg/kg, 50 mg/kg olaparib (oral, BID for 28 days) were tested in this model. Pamiparib induced tumor regression on day 29 and resulted in 100% objective responses (PR plus CR). At day 89, two months after treatment was terminated, tumor relapse was observed only in the lowest dose group (1.6 mg/kg); (B) all treatments had no effect on mouse body weight. (C) Dose-dependence of tumor PARylation inhibition and pamiparib plasma/tumor concentrations in the same model. Pamiparib induced a dose-dependent inhibition of PAR levels by 4 h after single oral administration of 0.17–10.9 mg/kg, which was correlated well with its PK in tumors; (D) time-dependence of PAR inhibition in tumors and its correlation with plasma/tumor PK. A single dose of 5.45 mg/kg pamiparib induced a rapid and potent decrease in PAR levels. The PARylation inhibition was 98% at 0.5 h and remained high ($\geq 80\%$) throughout the first 12 h; at 24 h post treatment, the inhibition remained at 53%. (E) The PARylation inhibited by pamiparib and olaparib were compared head-to-head. Compared to olaparib, pamiparib induced a more sustained PAR inhibition.

Table 2. Pamiparib and TMZ Combination in Glioblastoma and SCLC Cells.

Cell lines	EC ₅₀ of TMZ single agent (μM)	% of cells with EOB	Average EOB per cell	EC ₅₀ of TMZ + pamiparib @ nM (μM)	Max EC ₅₀ shift for TMZ	
GBM cell lines	SNB-19	>300	95%	34.7	9.1 μM@3μM	>33 fold ↓
	SF-295	>300	80%	36.9	10.5 μM@3μM	>29 fold ↓
	T98G	>300	55%	26.9	37.0 μM@3μM	>8 fold ↓
	SF-539	80	80%	19.9	10.2 μM@3μM	8 fold ↓
	U-118MG	>300	70%	24.0	42.0 μM@3μM	>7 fold ↓
	U251	32	80%	20.7	5.1 μM@3μM	6 fold ↓
	LN-229	>300	45%	10.6	55.2 μM@1μM	>5 fold ↓
	U87-MG	>300	50%	10.7	N.A.	N.A.
SCLC cell lines	NCI-H2227	576	75%	22.9	19.2 μM@3μM	30 fold ↓
	DMS153	60	35%	25.7	2.3 μM@3μM	26 fold ↓
	NCI-H1048	153	55%	18.6	6.3 μM@1μM	24 fold ↓
	NCI-H209	63	20%	4.6	13.8 μM@1μM	5 fold ↓
	NCI-H1436	>300	15%	~1.0	N.A.	N.A.
	NCI-H2286	182	25%	5.6	N.A.	N.A.
	NCI-H69	15	0	~13.8	N.A.	N.A.

cancer cell lines and 18 colorectal cancer (CRC) cell lines. Mild synergism effect was also observed in both cancer types, with an average EC₅₀s shift of TMZ of 4-fold decrease in CRC and 5.7-fold decrease in gastric cancer (Supplementary Table 2). These results clearly suggest a strong synergistic effect between pamiparib and TMZ. As TMZ is used for treating patients with brain cancer in clinic, we focused on GBM and SCLC models for further evaluation.

Next, to examine whether pamiparib can sensitize the TMZ-resistant cells, their combined activity was tested in a pair of H209 SCLC cell lines:

na \acute{Y} ve and TMZ-resistant H209 (H209-TR) cells. The H209-TR line was generated from H209 tumors by treatment with multiple cycles of TMZ *in vivo* and showed 3-fold greater resistance to TMZ than did the na \acute{Y} ve cell lines. Pamiparib was able to potentiate the effect of TMZ in both na \acute{Y} ve and H209-TR cells *in vitro* (Fig. 4A and 4B).

This observation was further confirmed in subcutaneous xenograft mouse models generated from na \acute{Y} ve and H209-TR cells. TMZ was effective at the beginning of the treatment in the na \acute{Y} ve H209 xenograft model: one cycle of the TMZ treatment resulted in all tumor-free animals.

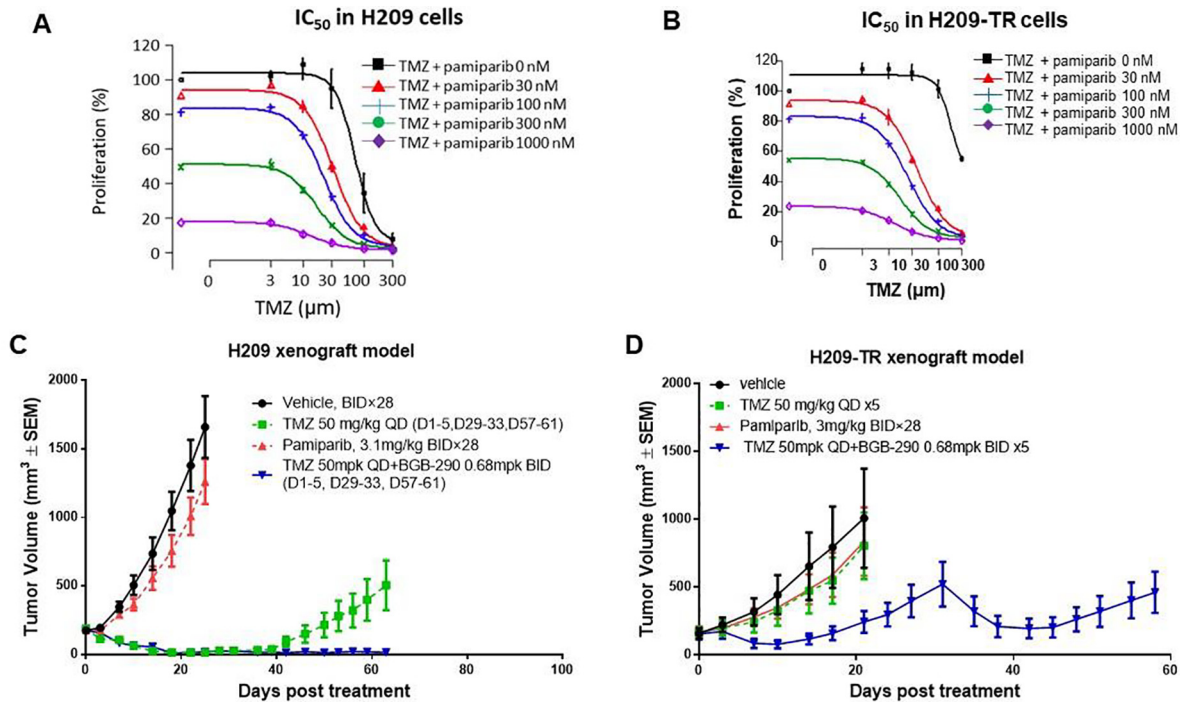


Fig. 4. Pamiparib potentiates temozolomide in both naive and TMZ-resistant H209 cells and in a xenograft mouse model. (A and B) IC_{50} curves in H209 and H209 TMZ resistance (H209-TR) cell lines. H209-TR cell lines were generated from H209 tumors by treatment with multiple cycles of TMZ *in vivo*. The derived H209-TR cells remained sensitive to the combination of pamiparib and TMZ *in vitro*. (C) The combined activity of pamiparib and TMZ in the H209 SCLC xenograft model. TMZ as a single agent was quite effective in this H209 model. One cycle of treatment resulted in all animals becoming tumor-free. However, resistance occurred quickly during the second cycle. Pamiparib and TMZ together significantly prevented resistance, and tumors remained sensitive to the drug combination after three cycles of 5-day treatment. (D) Synergistic activity of pamiparib and TMZ in the H209-TR xenograft model. TMZ single treatment was not effective in this model. In contrast, pamiparib and TMZ combination treatment was efficacious during two cycles of treatment.

However, resistance to TMZ developed quickly during the second cycle of the treatment. Combination of pamiparib with TMZ significantly reduced tumor recurrence, and tumors remained sensitive to the treatment after two cycles (Fig. 4C). However, in the H209-TR tumor models, TMZ single treatment showed no effect, while the combined pamiparib and TMZ treatment retained high efficacy for two treatment cycles (Fig. 4D). Taken together, these results establish that pamiparib exerts strong anti-tumor synergism with TMZ in both TMZ-sensitive and TMZ-resistant tumors.

Pamiparib exhibits strong brain penetration capacity and exerts anti-tumor synergism with TMZ in an SCLC intracranial model

Given that approximately 50% of SCLC patients have brain metastasis at the time of post mortem examination [31], and considering that TMZ is a frequent choice for treating such metastatic brain tumors in the clinic [32], the capability for pamiparib to penetrate the brain in mouse and rat models was further evaluated. First, a tissue distribution profile of pamiparib was determined in rats at 0.25, 1, 4, 8 and 24 h after a single oral administration at 5 mg/kg (Supplementary Table 3). At 24 h post treatment, the drug concentration in the brain was still high, at approximately 20% of the detected plasma level for the same time point, suggesting that pamiparib can successfully penetrate the BBB (Fig. 1 and Supplementary Table 3). This brain penetration capability was further confirmed in rats after a single I.V. dose of 1 mg/kg, with the mean K_{puu} of 15.8% indicating that pamiparib had marginal brain penetration potential (Supplementary Table 4). The brain penetration of pamiparib, along with four other PARP inhibitors was evaluated in male C57 mice after a single oral admin-

istration at their respective clinically relevant doses, except for olaparib, which followed the published preclinical dose [9,13,17,26,33]. The concentrations in brain and plasma were measured and their ratios were calculated at 1, 2, and 4 h (Table 3). Compared with talazoparib, olaparib, and niraparib, pamiparib resulted in the highest drug exposure in the brain, with the brain/plasma ratio around 20%, and maintaining the drug exposure in brain at this high level (i.e. >100 ng/g of drug concentration in brain, and ~19% of the brain/plasma ratio) for 4 h post treatment. These results suggest that pamiparib, as compared to other PARP inhibitors, has particularly strong BBB penetration activity in mice.

Next, an intracranial H209 xenograft was established as a model for SCLC brain metastasis in order to test the efficacy of the pamiparib and TMZ combination treatment. Pamiparib at 1.5 mg/kg (p.o.) showed significant penetration in this intracranial model, with a tissue/blood concentration ratio of 0.24 and 0.38 at 0.5- and 4-h post treatment, respectively (Fig. 5A). A single dose of pamiparib at 3 mg/kg (p.o.) induced complete inhibition of PARylation in brain tumors 4 h after treatment (Fig. 5B). Pamiparib monotherapy (3 mg/kg, BID, day 1–21, day 29–49) showed no significant effects in this model compared with the vehicle group (median survival 26.5 days vs. 24 days). Pamiparib significantly potentiated TMZ (TMZ 50 mg/kg plus pamiparib 0.75 mg/kg BID, day 1–15, 15–19, 29–33), leading to prolonged survival compared to a TMZ monotherapy (median survival 88 days vs. 75 days, $p < 0.05$) (Fig. 5C). The same treatment schedule was also tested in intracranial H209-TR xenografts. Tumors showed no response to TMZ monotherapy, with a median survival time of 24 days, compared with 22 days for the vehicle group. However, the combined pamiparib and TMZ treatment significantly prolonged survival, with a median survival of 56 days ($p < 0.01$). Thus, pamiparib

Table 3. Brain Penetration of PARP inhibitors in Mice.

Dose of Compound		AUC _{1-4h} (ng/ml*h or ng/g*h)	Plasma(ng/mL) or Brain(ng/g) Concentration		
			1 h	2 h	4 h
Pamiparib 10 mg/kg, p.o.	Plasma	4470	3527	1333	707
	Brain	820	613	252	135
	Brain/Plasma (%)	18%	17%	19%	19%
Talazoparib 3 mg/kg, p.o.	Plasma	5628	3276	2115	817
	Brain	85	16	34	26
	Brain/Plasma (%)	2%	0%	2%	3%
Olaparib 50 mg/kg, p.o.	Plasma	3160	3273	771	366
	Brain	56	45	17	9
	Brain/Plasma (%)	2%	1%	2%	2%
Niraparib 50 mg/kg, p.o.	Plasma	20,214	7385	7021	5990
	Brain	1849	428	549	812
	Brain/Plasma (%)	9%	6%	8%	14%

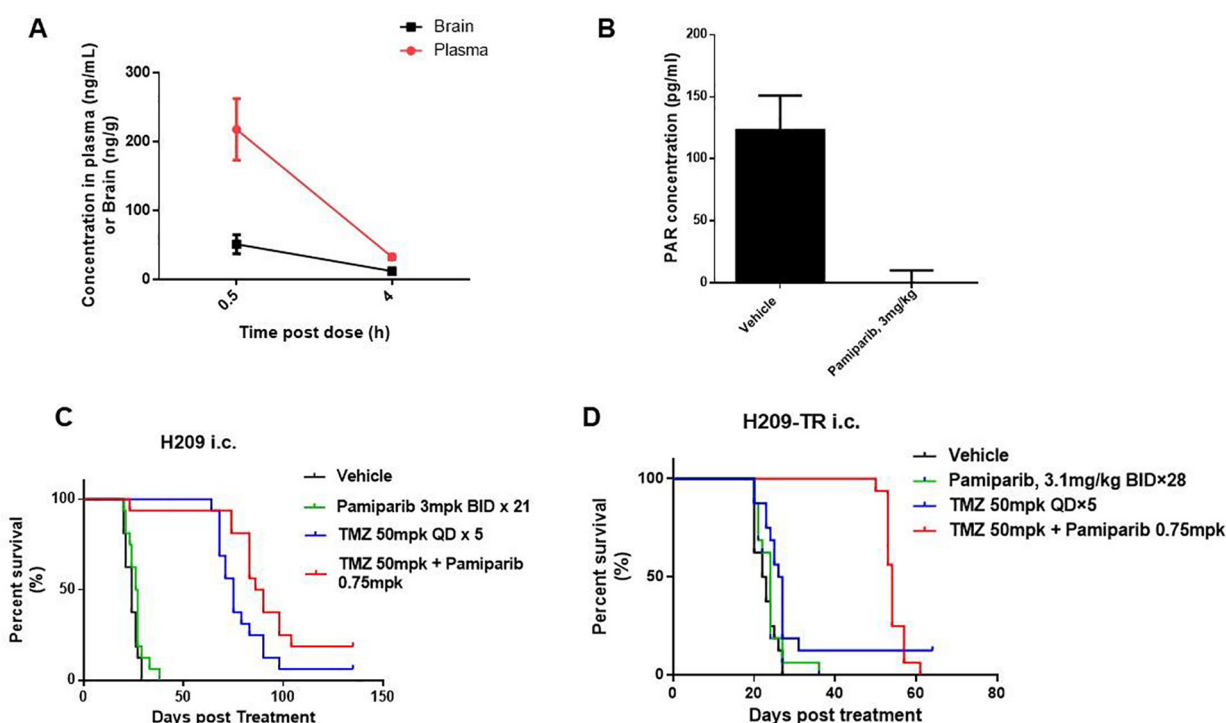


Fig. 5. Brain penetration of pamiparib and its efficacy combined with TMZ in an intracranial H209 xenograft model. (A) Brain penetration of pamiparib in an intracranial H209 xenograft at 1.5 mg/kg p.o. (B) PD activity of pamiparib in the intracranial model, PARylation in brain/tumor was completely inhibited at 4 h after a single dose of 3 mpk p.o. (C and D) The synergistic activity of pamiparib and TMZ in H209 and H209-TR intracranial xenograft. TMZ and the combination treatment of TMZ and pamiparib showed no significant difference in survival in the H209 naïve model. However, the combination treatment of TMZ and pamiparib dramatically prolonged the survival of the H209-TR models. The survival time was defined as the time from the day of tumor cell inoculation to one day before animal death or euthanization. Kaplan–Meier curves were generated using mouse survival duration in days.

exhibits strong BBB penetration, which apparently potentiates TMZ efficacy in SCLC brain metastasis models.

Besides this, the combo effect of TMZ and pamiparib was also evaluated in GL261 syngeneic intracranial glioma models. Single agent of pamiparib at 9 mpk has no efficacy at all with the median survival of 21 days versus 22 days in the vehicle-treated group. However, TMZ in combination with pamiparib resulted in significantly extended survival comparing with TMZ alone (Supplementary Fig. 4). These data strongly support that TMZ and pamiparib exert excellent efficacy in brain tumors, both primary and metastasis settings.

Discussion

In this report, we presented evidence showing that pamiparib, a selective PARP1/2 inhibitor, has potent DNA-trapping and anti-proliferation activity against several human cancer cell lines harboring BRCA1/2 mutations or HRD. Oral administration of pamiparib demonstrated high bioavailability in mice and other species tested (Table 1). In MDA-MB-436 breast cancer xenografts in mice, oral administration of pamiparib resulted in time- and dose-dependent inhibition of PARylation, and exhibited high efficacy for inducing significant, dose-dependent decreases in

tumor size. Furthermore, pamiparib also showed strong synergism with TMZ both *in vitro* and *in vivo*. Pamiparib effectively potentiated TMZ in brain tumors, both GBM and SCLC intracranial xenografts, likely owing to its capacity to penetrate the BBB. In summary, these data demonstrate that pamiparib has strong anti-tumor activity, both as a single agent or in combination with TMZ, in multiple tumor models.

PARP inhibitors, such as olaparib, have been demonstrated to have monotherapy activity against tumor cells harboring BRCA1 or BRCA2 mutations, exerting effects via synthetic lethality interactions [6–8]. Tumor cells with a compromised HR pathway are known to be susceptible to becoming highly dependent upon PARP activity for maintaining the genomic integrity and survival, even in the cells without BRCA1/2 mutations [34]. Similar to other PARP inhibitors, pamiparib was found to show strong inhibitory activities with a selectivity to the BRCA1/2 mutation or HRD cancer cells. Specifically, head-to-head comparisons with olaparib revealed comparable antiproliferative activity—with a similar mechanism of action—against multiple tumor cell lines with known HRD, including MDA-MB-436, HCC1395, UWB1.289, and HCT116/ATR(-/flox). Such pamiparib-induced tumor cell inhibition was not observed in cell lines lacking HRD.

In addition to inhibition of PARylation, DNA trapping by the PARP inhibitor complex is another major mechanism through which PARP inhibitors induce cytotoxicity in tumor cells. PARP detects and localizes to DNA SSB to facilitate its repair, which then potentiates the recruitment of DNA SSB repair proteins to the chromatin and promotes the dissociation of PARP itself from the DNA [35]. PARP inhibition therefore traps PARP on the DNA at the sites of unrepaired SSBs, resulting in the generation of DNA double-strand breaks in S-phase which further requires a functional HR pathway for successful repair [36,37]. Pamiparib was demonstrated potent DNA-trapping activity (with an EC₅₀ of 13 nM) at a level comparable to olaparib but was 30-fold more potent than veliparib, in the biochemical assays.

Besides *in vitro* potency, pamiparib showed greater potency than olaparib *in vivo*. Based on dose titration or time-dependent PD studies, as well as efficacy studies (Fig. 3), a simple PK/PD model was established to understand the relationship between pamiparib dose concentrations and efficacy. The model suggested that an intra-tumor concentration of >0.5 μmol/kg is required to achieve at least 80% PARylation inhibition by pamiparib, and BID dosing is required to sustain the PD effect in mice. Further, our head-to-head PD and efficacy comparison studies showed that pamiparib induced a more sustained PAR inhibition compared with olaparib. Thus, pamiparib exhibits approximately 16-fold higher efficacy than olaparib in this model, likely due to higher drug exposure in plasma or at tumor sites.

TMZ is a DNA alkylating agent which is used for treating several malignancies, including GBM and SCLC with brain metastasis [18,38]. TMZ-mediated DNA damage is repaired by the BER pathway, for which PARP enzymes are required [21]. Therefore, PARP inhibition may enhance TMZ cytotoxicity by preventing BER pathway-mediated repair of base lesions [22,23]. We demonstrated that pamiparib can enhance the anti-tumor effect of TMZ in both primary and metastatic brain tumors. Besides this, pamiparib can reverse TMZ-resistant SCLC H209 xenografts' response to TMZ with stronger and extended efficacy. Our study establishes that pamiparib and TMZ together exhibit strong synergistic effects *in vivo* and *in vitro*, with both TMZ naïve and resistant cell lines (Fig. 4). Interestingly, a significant brain penetration by pamiparib was observed both in rat and mice, supporting its strong utility as a combination agent with TMZ for treatment of brain tumors or tumors with brain metastasis.

The BBB is the main hurdle for xenobiotics to exert CNS effects. In addition to brain cell tight junctions, efflux transporters such as P-gp and BCRP highly expressed at the luminal membrane of endothelial cells transport a diverse range of lipid-soluble compounds out of the brain's

capillary endothelium, thereby limiting the ability of such substances to accumulate in brain parenchyma [39]. A rational design strategy for CNS compounds would therefore prefer a non-P-gp and BCRP substrate profile. Indeed, pamiparib is not a substrate of P-gp or BCRP (Supplementary Table 5). In contrast, several studies have revealed that previous generation PARP inhibitors like olaparib, rucaparib, talazoparib, and veliparib have significant MDR1 or P-gp efflux liability, which may restrict their delivery across the BBB [25,26]. Furthermore, the combination of pamiparib and TMZ significantly prolonged animal survival compared to TMZ as a single agent in TMZ-resistant SCLC intracranial xenograft models.

Given our observation of strong BBB penetration and strong synergistic activity, further clinical development of combined treatments comprising pamiparib alongside TMZ in patients with brain malignancies, especially those who develop TMZ resistance, are also warranted. Pamiparib can serve as an excellent candidate for clinical trials. In fact, preliminary clinical data has already demonstrated the safety and efficacy of pamiparib in patients with BRCA or HRD [40], and clinical development of a combination therapy of pamiparib together with TMZ is currently underway [NCT03150862].

Beyond olaparib's poor BBB penetration, another clinical limitation is that the action of P-gp and BCRP drastically reduces olaparib's efficacy by causing patient resistance [41,42]. Novel mechanisms of drug resistance in ovarian cancer have been identified, including genetic mutations that result in the activation of a drug efflux pump or secondary mutations in BRCA1/2 genes that restore the cancer cell's ability to repair treatment related DNA damage [43]. Notably, as a non-substrate of P-gp or BCRP, pamiparib might overcome the resistance caused by over-expression of P-gp and BCRP. Thus, we hypothesize that patients with BRCA1/2 mutant high grade serous ovarian cancer or carcinosarcoma who have progressed on recent therapy and have an activated efflux pump without a secondary BRCA1/2 mutation will be particularly suitable for pamiparib. This hypothesis is currently being tested in a clinical trial [NCT03933761].

Disclosure of potential conflicts of interest

All authors, besides Yiyuan Wu and Zhen Qin, have ownership interest in BeiGene.

Yiyuan Wu and Zhen Qin are former employees of BeiGene.

Hexiang Wang, Bo Ren, and Changyou Zhou are inventors on a patent covering Pamiparib described in this study.

Appendix A. Supplementary data

Supplementary data to this article can be found online at <https://doi.org/10.1016/j.neo.2020.06.009>.

References

- Hanahan D, Weinberg RA. Hallmarks of cancer: the next generation. *Cell*. 2011;144(5):646–74. <https://doi.org/10.1016/j.cell.2011.02.013>.
- Li X, Heyer WD. Homologous recombination in DNA repair and DNA damage tolerance. *Cell Res*. 2008;18(1):99–113. <https://doi.org/10.1038/cr.2008.1>.
- Narod SA, Foulkes WD. BRCA1 and BRCA2: 1994 and beyond. *Nat Rev Cancer* 2004;4:665–76. <https://doi.org/10.1038/nrc1431>.
- Rouleau M, Patel A, Hendzel MJ, et al. PARP inhibition: PARP1 and beyond. *Nat Rev Cancer* 2010;10(4):293–301. <https://doi.org/10.1038/nrc2812>.
- Lord CJ, Ashworth A. PARP inhibitors: synthetic lethality in the clinic. *Science*. 2017;355(6330):1152–8. <https://doi.org/10.1126/science.aam7344>.
- Audeh MW et al. Oral poly(ADP-ribose) polymerase inhibitor olaparib in patients with BRCA1 or BRCA2 mutations and recurrent ovarian cancer: a

- proof-of-concept trial. *Lancet*. 2010;**376**(9737):245–51. [https://doi.org/10.1016/S0140-6736\(10\)60893-8](https://doi.org/10.1016/S0140-6736(10)60893-8).
7. Fong PC, Boss DS, Yap TA, et al. Inhibition of poly(ADP-ribose) polymerase in tumors from BRCA mutation carriers. *N Engl J Med* 2009;**361**(2):123–34. <https://doi.org/10.1056/NEJMoa0900212>.
 8. Fong PC, Yap TA, Boss DS, et al. Poly(ADP)-ribose polymerase inhibition: frequent durable responses in BRCA carrier ovarian cancer correlating with platinum-free interval. *J Clin Oncol* 2010;**28**(15):2512–9. <https://doi.org/10.1200/JCO.2009.26.9589>.
 9. Gelmon KA, Tischkowitz M, Mackay H, et al. Olaparib in patients with recurrent high-grade serous or poorly differentiated ovarian carcinoma or triple-negative breast cancer: a phase 2, multicentre, open-label, non-randomised study. *Lancet Oncol* 2011;**12**(9):852–61. [https://doi.org/10.1016/S1470-2045\(11\)70214-5](https://doi.org/10.1016/S1470-2045(11)70214-5).
 10. Bryant HE, Schultz N, Thomas HD, et al. Specific killing of BRCA2-deficient tumours with inhibitors of poly(ADP-ribose) polymerase. *Nature* 2005;**434**(7035):913–7. <https://doi.org/10.1038/nature03443>.
 11. Farmer H, McCabe N, Lord CJ, et al. Targeting the DNA repair defect in BRCA mutant cells as a therapeutic strategy. *Nature* 2005;**434**(7035):917–21. <https://doi.org/10.1038/nature03445>.
 12. Satoh MS, Lindahl T. Role of poly(ADP-ribose) formation in DNA repair. *Nature* 1992;**356**(6367):356–8. <https://doi.org/10.1038/356356a0>.
 13. Litton JK, Rugo HS, Ettl J, et al. Talazoparib in patients with advanced breast cancer and a germline BRCA mutation. *N Engl J Med* 2018;**379**(8):753–63. <https://doi.org/10.1056/NEJMoa1802905>.
 14. Brown JS, Kaye SB, Yap TA. PARP inhibitors: the race is on. *Br J Cancer* 2016;**114**(7):713–5. <https://doi.org/10.1038/bjc.2016.67>.
 15. Mateo J, Lord CJ, Serra V, et al. A decade of clinical development of PARP inhibitors in perspective. *Ann Oncol* 2019;**30**(9):1437–47. <https://doi.org/10.1093/annonc/mdz192>.
 16. Shapiro G, Kristeleit R, Middleton M, et al. Pharmacokinetics of orally administered rucaparib in patients with advanced solid tumors. *Mol Cancer Ther*, 2013;12(11 Suppl): Abstract nr A218. DOI: 10.1158/1535-7163.
 17. Michie CO, Sandhu SK, Schelman WR, et al. Final results of the phase I trial of niraparib (MK4827), a poly(ADP)ribose polymerase (PARP) inhibitor incorporating proof of concept biomarker studies and expansion cohorts involving BRCA1/2 mutation carriers, sporadic ovarian, and castration resistant prostate cancer (CRPC). *J Clin Oncol*, 2013;31(suppl; abstr 2513). DOI:10.1200/jco.2013.31.15_suppl.2513.
 18. Molla S, Hembram KC, Chatterjee S, et al. PARP inhibitor olaparib enhances the apoptotic potentiality of curcumin by increasing the DNA damage in oral cancer cells through inhibition of BER cascade. *Pathol Oncol Res* 2019. <https://doi.org/10.1007/s12253-019-00768-0>.
 19. Gerson SL. Clinical relevance of MGMT in the treatment of cancer. *J Clin Oncol* 2002;**20**(9):2388–99. <https://doi.org/10.1200/JCO.2002.06.110>.
 20. Esteller M, Herman JG. Generating mutations but providing chemosensitivity: The role of O6-methylguanine DNA methyltransferase in human cancer. *Oncogene* 2004;**23**(1):1–8. <https://doi.org/10.1038/sj.onc.1207316>.
 21. Pietanza MC, Waqar SN, Krug LM, et al. Randomized, double-blind, phase II study of temozolomide in combination with either veliparib or placebo in patients with relapsed-sensitive or refractory small-cell lung cancer. *J Clin Oncol* 2018;**36**(23):2386–94. <https://doi.org/10.1200/JCO.2018.77.7672>.
 22. Gupta SK, Kizilbash SH, Carlson BL, et al. Delineation of MGMT hypermethylation as a biomarker for veliparib-mediated temozolomide-sensitizing therapy of glioblastoma. *J Natl Cancer Inst* 2016;**108**(5):1–10. <https://doi.org/10.1093/jnci/djv369>.
 23. Barazzuol L, Jena R, Burnet NG, et al. Evaluation of poly (ADP-ribose) polymerase inhibitor ABT-888 combined with radiotherapy and temozolomide in glioblastoma. *Radiat Oncol* 2013;**8**:65. <https://doi.org/10.1186/1748-717X-8-65>.
 24. de Gooijer MC, Buil LCM, 'itirikaya CH, et al. ABCB1 attenuates the brain penetration of the PARP inhibitor AZD2461. *Mol Pharm* 2018;**15**(11):5236–43. <https://doi.org/10.1021/acs.molpharmaceut.8b00742>.
 25. Durmus S, Sparidans RW, van Esch A, et al. Breast cancer resistance protein (BCRP/ABCG2) and P-glycoprotein (P-GP/ABCB1) restrict oral availability and brain accumulation of the PARP inhibitor rucaparib (AG-014699). *Pharm Res* 2015;**32**(1):37–46. <https://doi.org/10.1007/s11095-014-1442-z>.
 26. Kizilbash SH, Gupta SK, Chang K, et al. Restricted delivery of talazoparib across the blood-brain barrier limits the sensitizing effects of PARP inhibition on Temozolomide therapy in glioblastoma. *Mol. Cancer Ther* 2017;**16**:2735–46. <https://doi.org/10.1158/1535-7163>.
 27. Mendes-Pereira AM, Martin SA, Brough R, et al. Synthetic lethal targeting of PTEN mutant cells with PARP inhibitors. *EMBO Mol Med* 2009;**1**(6–7):315–22. <https://doi.org/10.1002/emmm.200900041>.
 28. Stupp R, Mason WP, van den Bent MJ, et al. Radiotherapy plus concomitant and adjuvant temozolomide for glioblastoma. *N Engl J Med* 2005;**352**(10):987–96. <https://doi.org/10.1056/NEJMoa043330>.
 29. Pietanza MC, Kadota K, Huberman K, et al. Phase II trial of temozolomide in patients with relapsed sensitive or refractory small cell lung cancer, with assessment of methylguanine-DNA methyltransferase as a potential biomarker. *Clin Cancer Res* 2012;**18**(4):1138–45. <https://doi.org/10.1158/1078-0432.CCR-11-2059>.
 30. Bansal M, Yang J, Karan C, et al. A community computational challenge to predict the activity of pairs of compounds. *Nat Biotechnol* 2014;**32**(12):1213–22. <https://doi.org/10.1038/nbt.3052>.
 31. Quan AL, Videtic GMM, Suh JH. Brain metastases in small cell lung cancer. *Oncology (Williston Park)* 2004;**18**(8):961–72.
 32. Walbert T, Gilbert MR. The role of chemotherapy in the treatment of patients with brain metastases from solid tumors. *Int J Clin Oncol* 2009;**14**(4):299–306. <https://doi.org/10.1007/s10147-009-0916-1>.
 33. Kortmann U, McAlpine JN, Xue H, et al. Tumor growth inhibition by Olaparib in BRCA2 germline-mutated patient derived ovarian cancer tissue xenografts. *Clin Cancer Res* 2010;**4**(17):783–91. <https://doi.org/10.1158/1078-0432>.
 34. Sztupinski Z, Diossy M, Krzystanek M, et al. Detection of molecular signatures of homologous recombination deficiency in prostate cancer with or without BRCA1/2 mutations. *Clin Cancer Res* 2020. <https://doi.org/10.1158/1078-0432.CCR-19-2135>.
 35. Pommier Y, O'Connor MJ, de Bono J. Laying a trap to kill cancer cells: PARP inhibitors and their mechanisms of action. *Sci Transl Med* 2016;**8**(362):362ps17. <https://doi.org/10.1126/scitranslmed.aaf9246>.
 36. Helleday T. The underlying mechanism for the PARP and BRCA synthetic lethality: clearing up the misunderstandings. *Mol Oncol*, 2011;594: 387–93. DOI: 10.1016/j.molonc.2011.07.001.
 37. O'Connor MJ. Targeting the DNA damage response in cancer. *Mol Cell* 2015;**60**(4):547–60. <https://doi.org/10.1016/j.molcel.2015.10.040>.
 38. Yung WK, Albright RE, Olson J, et al. A phase II study of temozolomide vs. procarbazine in patients with glioblastoma multiforme at first relapse. *Br J Cancer* 2000;**83**(5):588–93. <https://doi.org/10.1054/bjoc.2000.1316>.
 39. Abbott NJ, Patabendige AAK, Dolman DEM, et al. Structure and function of the blood-brain barrier. *Neurobiol Dis* 2010;**37**(1):13–25. <https://doi.org/10.1016/j.nbd.2009.07.030>.
 40. Wu X, Wang J, Zhou Q, et al. Pamiparib, a novel PARP 1/2 inhibitor, monotherapy for gBRCAm patients with recurrent ovarian, fallopian, and primary peritoneal cancer: An open-label, multicenter, phase II trial in China. *Ann Oncol* 2018;**29**(8):viii356. <https://doi.org/10.1093/annonc/mdy285.205>.
 41. Henneman L, van Miltenburg MH, Michalak EM, et al. Selective resistance to the PARP inhibitor olaparib in a mouse model for BRCA1-deficient metaplastic breast cancer. *Proc Natl Acad Sci U S A* 2015;**112**(27):8409–14. <https://doi.org/10.1073/pnas.1500223112>.
 42. Dufour R, Daumar P, Mounetou E, et al. BCRP and P-gp relay overexpression in triple negative basal-like breast cancer cell line: a prospective role in resistance to Olaparib. *Sci Rep* 2015;**5**:12670. <https://doi.org/10.1038/srep12670>.
 43. Kubalanza K, Konecny GE. Mechanisms of PARP inhibitor resistance in ovarian cancer. *Curr Opin Obstet Gynecol* 2020;**32**(1):36–41. <https://doi.org/10.1097/GCO.0000000000000600>.